

Characterizing Porous Ceramics by Frequency-Response Method

M. Järveläinen* T. Salpavaara**
S. Seppälä* T. Roinila** T. Yli-Hallila**
E. Levänen* M. Vilkkö**

*Department of Materials Science, Tampere University of Technology, P.O. Box 589, FI-33101 Tampere, Finland

** Department of Automation Science and Engineering, Tampere University of Technology, P.O. Box 692, FI-33101 Tampere, Finland

Abstract: Nondestructively determining pore properties of ceramic materials is essential in many industrial applications. There are several limitations in the existing characterization methods, so new techniques are required to meet the increasing demands of analysis. This paper examines the possible use of an electrical frequency-response method based on broadband excitation and Fourier techniques to characterize porous ceramic materials. The applied method provides a non-destructive, online characterization technique that is fast and can be applied inexpensively. In this article, ceramic samples with three different pore characteristics were measured by the frequency-response method that used a pseudo-random binary sequence. A sample of material was placed between the plates of a capacitor, and the capacitance was measured. Material properties, such as porosity, influence the permittivity value of the material. The samples with different porosities can be distinguished by analyzing the capacitance of the capacitor.

Keywords: capacitors, characterization, density measurements, frequency-response methods, impulse signals, permittivity, polarization analysis, pseudo random sequences, signal detection

1. INTRODUCTION

The number of ceramic materials used in functional and construction applications in industrial environments is continuously increasing. The main reason is their attractive properties, such as high temperature, chemical resistance, hardness, and the potential to easily tailor the pore characteristics in a controlled manner. Ceramic materials are used in critical process components in challenging environments, such as in the presence of corrosive acids and bases, because no other material can withstand the challenging atmospheres.

This study aims to develop a fast, continuous, online, and onsite pore characterization method, based on frequency-response measurements for ceramic materials in industrial applications. Traditional, nondestructive testing methods have limitations, such as cost, sample size, and slowness, so there is a strong need for the frequency-response technique. In an industrial process, this could mean improving quality control, safety, and efficiency. In addition to porosity measurements, this method could have other interesting applications. Porosity influences other important properties of ceramics, such as modulus of elasticity (Asmaniet al. 2001), strength (Coble et al. 1956), and thermal insulation ability (Sumirat et al. 2006). Furthermore, porosity has a functional purpose in many applications (Studart et al. 2006), such as ceramic bio-implants (Kamitakahara et al. 2008, Niemelä et al. 2011), membranes (Ciora et al. 2003, Garmash et al. 1995), drug delivery (Ahuja et al. 2009), solid oxide fuel cells (Sanson et al. 2008), and absorbent structures (Ojuva et al. 2013, Vasiliev et al. 2010).

The frequency-response method in this article is an electrical porosity measurement based on different polarization behaviors of materials in alternating electric fields. As Lira-Olivares et al. (2000) stated the following polarization types are encountered in ceramics: Electronic, ionic, dipolar orientation, and Maxwell-Wagner-Sillars (Lira-Olivares et al., 2000). According to Richerson (2006), atoms and their bonding types affect material polarization sensitivity and rate (Richerson, 2006). These physical phenomena should enable discrimination of two phases by analyzing the disturbances in a sample polarity. The applicability of the frequency-response method in porosity measurements is studied by measuring the behavior of ceramic materials in alternating electric fields. Vila et al. (1998) found that porosities and impurities in ceramics influence measured permittivity and dielectric loss (Vila et al., 1998). This study clarifies how changes in porosity, such as differences in amounts of air and solids, affect the measured electrical properties.

The proposed frequency-response analytical method has several attractive features, such as flexibility in industrial applications, fastness, size scaling, and potential use as a non-destructive online tool. An electrical impulse, required as an excitation signal, is easy and straightforward to generate and use. Calculating the responses is based on simple Fourier techniques so are easy to implement in practice. We used a maximum-length binary sequence (MLBS) excitation to quickly measure a wide frequency band of materials. The MLBS excitation method is interesting because the energy density of the excitation is very even across the whole measuring range. In addition, because the MLBS has only two different signal values, it can be easily implemented with a low-cost application.

There are no existing methods that fulfill all the above-mentioned requirements. Mercury porosimetry (Giesche, 2006) analyzes small sample sizes and is destructive. Computed tomography (Taud et al. 2005) and magnetic resonance imaging (Fagan et al. 2005) are non-destructive, but measurements are slow. The same applies to gas-adsorption methods (Sing et al. 1985). The traditional Archimedes method can be used for big samples, but the measurement is time consuming and laborious. None of these methods can be used for continuous analysis.

2. METHODS AND MATERIALS

For the frequency-response measurement, samples were manufactured and characterized by Archimedes measurement. This section is divided into three parts. The first part considers the sample manufacturing and characterization, the second part considers signal generation, and the last part considers the applied equipment and the idea of the electrical frequency-response method.

2.1 Manufacturing and characterization of alumina samples

To study the functionality and sensitivity of the frequency-response method to measure porosity, ceramic sample series with various porosity properties were manufactured and characterized by the Archimedes method. Samples were made of aluminum oxide (alumina), because it is a common technical ceramic with well-known properties. Alumina has high resistivity and is an electrical insulator. Microstructure and impurities affect the electrical properties of alumina.

The sample series were manufactured by slip casting. By using three different sintering temperatures, samples with three different porosities were achieved.

Slip casting of alumina samples. In slip casting, a ceramic component is produced from a slip containing ceramic powder, water, and additives. First a dispersing agent (Dispex A40) was stirred into the water. The dispersing agent worked as a stabilizer in the slip. Then alumina powder (Al_2O_3 , Martinswerk MR70) was added to the mixture. After the powder was stirred until it was homogenous, a binder (Raisional 116) was added to increase pre-sintering strength of the component. Finally, polyethylene glycol was stirred into the slip to increase processability.

The prepared slip was poured into a gypsum mold, where the solid content compacted to the mold walls as water was removed by capillary action. When the component was solidified, the mold was removed. Before sintering, the component is known as a green body. To avoid cracking, the green body was dried before sintering for 24 hours at 45°C, followed by 24 hours at 90°C.

Sintering. After drying and processing, the green bodies were heated at high temperatures, where the structure of the ceramics became denser due to diffusion of atoms. This is called *sintering*. This also caused the component to shrink. We selected three different sintering temperatures: 1100°C, 1300°C, and 1550°C. Heat treatment was carried out in two steps. First, the green bodies were heated at 1°C/min up to 200°C, with a 60-minute dwell. The ceramics were then heated at 1°C/min up to the sintering temperature, with a 120-

minute dwell. The cooling rate after heating was 5°C/minute. After sintering, the samples were characterized by the Archimedes method. Microstructures were studied by scanning electron microscopy (SEM) (Phillips XL-30).

Material characterization. Density and porosity properties of the samples were determined by the Archimedes method. The test was performed according to ASTM standard (ASTM Standard C373-88) to four representative samples from each sintering temperature. The test measured dry mass, saturated mass, and mass when the sample was suspended in water. From these values, porosities and densities were determined. Average values of the results are presented in Table 1. A theoretical density of 3.98g/cm³ was used in the calculations.

Table 1. Results of Archimedes test; porosity properties of the samples.

Sintering temperature [°C]	Bulk density [g/cm ³]	Apparent density [g/cm ³]	Open porosity [%]	Total porosity [%]
1550	3.85	3.86	0.09	3.23
1300	3.27	3.89	15.78	17.94
1100	2.66	3.89	31.62	33.10

In addition to the Archimedes test, the samples were imaged by SEM. The samples were cut, ground, and polished. Fig. 1 shows the sintering shrinkages and microstructures of cross-sectional areas.

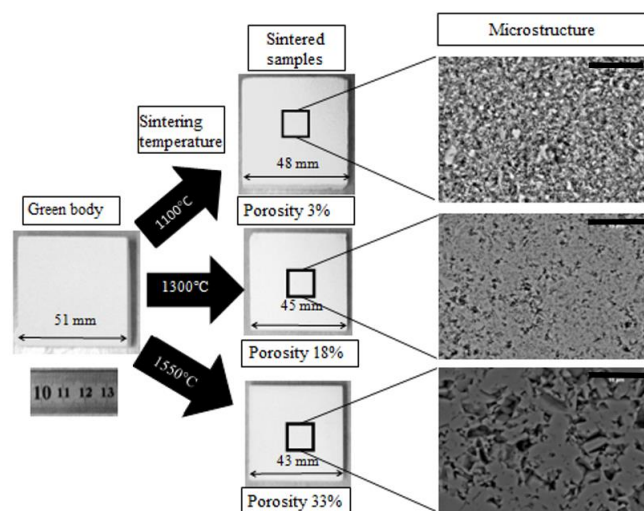


Fig. 1. Sample in green state and after sintering. The length of the black scale bars in the SEM-photos is 10 μm.

2.2 Frequency-response measurement

In steady state, for small-signal disturbances, the analyzed system is linear and time-invariant. According to basic control theory, this type of system is fully characterized by its impulse response in the time domain, which can be transformed to the frequency domain and presented as a frequency-response function.

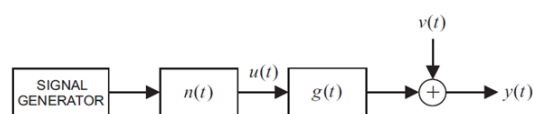


Fig. 2. Typical frequency-response-measurement setup.

Fig. 2 shows a typical frequency-response-measurement setup, in which the device under test, presented by the system impulse-response function $g(t)$, is to be identified. The designed excitation is first processed (filtered and amplified by $n(t)$), yielding the actual excitation $u(t)$. The device under test is then perturbed with $u(t)$, yielding the corresponding output response $y(t)$. The measured signal is corrupted with noise, presented by $v(t)$. The noise resembles white noise and is uncorrelated with $u(t)$ and $y(t)$. All the signals are assumed to be zero-mean sequences. Applying cross correlation between the sampled input and output responses, an estimate of the frequency-response function is obtained as:

$$G(e^{j\omega T_s}) = \frac{1}{\alpha} \sum_{k=0}^{M-1} R_{uy}(m) e^{-jk\omega T_s} \quad (1)$$

where M , α , T_s , and $R_{uy}(m)$ respectively denote the total length of collected data, the variance of $u(m)$, the sampling interval, and the cross-correlation function between the input and output signals (James, 2004). The requirement in (1) is that the system is perturbed with a signal resembling white noise, such as with maximum-length binary sequence (MLBS) (Godfrey, 1993). Other frequency-response-computation techniques can be found (e.g., Pintelon et al., 2001).

2.3 Maximum-length binary sequence

Pseudo-random binary sequence (PRBS) is a periodic broadband signal with the following properties:

1. The signal has two levels and can switch the level only at certain event points $t = 0, \Delta t, 2\Delta t, \dots$
2. The change of signal level is predetermined, so that PRBS is deterministic and experiments are repeatable.
3. The sequence is periodic with period $T = N\Delta t$, where N is an odd integer
4. Within one period, there are $(N + 1)/2$ intervals when the signal is at one level and $(N - 1)/2$ intervals when it is at the other.

A PRBS is based on a sequence of length N . The most commonly used signals are based on maximum-length sequences (maximum-length binary sequence [MLBS]). Such sequences exist for $N = 2^n - 1$, where n is an integer. They are popular because they can be generated using feedback shift register circuits, as shown in Fig. 3.

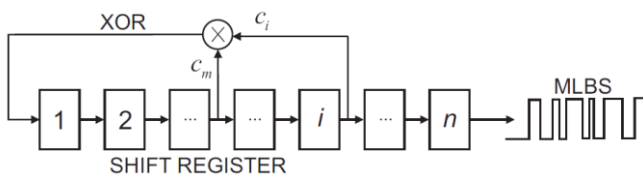


Fig. 3. N -bit shift register with XOR feedback for MLBS generation.

Table 2 shows an example of an output from a shift register circuit for generating an MLBS of length $2^4 - 1 = 15$. The feedback is generated from stages 1 and 4. All four columns in Table 1 produce the same MLBS. The register can be started with any number other than 0,0,0,0. In the example, the register starts from 0,0,0,1. Each binary number from 0,0,0,1 to 1,1,1,1 appears exactly once (the sequence starts repeating after 15 cycles). This is a general result for all MLBS (Godfrey, 1993). In practice, the values 0 and 1 are mapped to -1 and +1 to produce a symmetrical MLBS with an average close to zero.

Table 2: Maximum-length binary sequence from a four-stage shift register.

Shift	Stage 1	Stage 2	Stage 3	Stage 4
1	0	0	0	1
2	1	0	0	0
3	1	1	0	0
4	1	1	1	0
5	1	1	1	1
6	0	1	1	1
7	1	0	1	1
8	0	1	0	1
9	1	0	1	0
10	1	1	1	1
11	0	1	1	0
12	0	0	0	1
13	1	0	0	1
14	0	1	1	0
15	0	0	0	0
16	0	0	0	1

Selection of the feedback connections (stages) is important. Very few of the possible connections result in a sequence of the maximum length $2^n - 1$ (some sequences can be produced from several different stages). The linear feedback shift register can be described by a polynomial. The polynomial has a degree that equals the length of the register and has coefficients that are either 0 or 1 (depending on the applied stages). For example, the polynomial of the 15-bit-length MLBS (4-bit-length shift register) shown in Table 1 has a polynomial $x^4 + x + 1$ (the applied stages are 1 and 4; the 1 corresponds to the input of the first bit). A necessary, sufficient condition for the sequence to be maximal length is that the corresponding polynomial is primitive.

Fig. 4 shows the form of the power spectrum of the MLBS shown in Table 1. The sequence is generated at 10 kHz and has signal levels ± 1 V. The power spectrum has an envelope and drops to zero at the generation frequency and its harmonics. The spectrum is given by

$$\Phi_{\text{MLBS}}(q) = \frac{a^2 (N+1) \sin^2(\pi q / N)}{N^2 (\pi q / N)^2}, \quad q = \pm 1, \pm 2, \dots \quad (2)$$

where q denotes the sequence number of the spectral line, a is the signal amplitude, and N is the signal length.

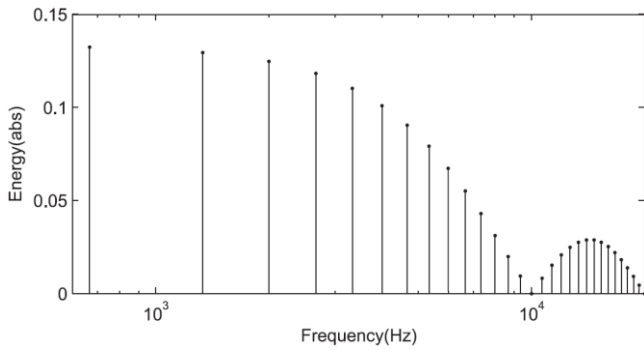


Fig. 4. Power spectrum of 15-bit-length MLBS generated at 10 kHz.

The MLBS x has the lowest possible peak factor $|x|_{peak}/x_{rms} = 1$ regardless of its length. Therefore, the sequence is well-suited for sensitive systems that require small-amplitude perturbation. Due to the deterministic nature of the sequence, the signal can be repeated and injected precisely, and the SNR can be increased by synchronous averaging of the response periods. Other advantages of the MLBS method include straightforward generation and design of the sequence. Because the MLBS has only two signal values, it can be generated with a low-cost application, the output of which can only cope with a small number of signal levels. This is not the case with multi-sine signals, which have an infinite number of signal levels.

2.4 Measurement system

The method for measuring porosity was based on the electric frequency-response measurement described in Section 2.2. The porosity affects the permittivity of a sample, altering the frequency response of the system. The required electronics of the measurement system were kept as simple as possible. The system was built to interface with National Instrument's PCI-6052E measurement card. The measurement card sent and measured an excitation of the system and also received the output signal of the system. The measurement system consisted of a resistor and a capacitor that formed a first-order low-pass-filter, presented in Fig. 5. The capacitor was designed so that the sample could be inserted between the capacitor plates in a controlled manner.

In the measurement, a sample was placed between the capacitor plates as a dielectric so that the relative permittivity of the sample affected the capacitor's capacitance. The ceramic samples were 12 mm thick and placed on a 3x3 cm electrode area that was made of circuit-board material. A ground plane was put on top of the sample. There was another ground plane under the electrode area on the other side of the capacitor plane. Due to the measurement arrangements, the total capacitance of the system consisted of both the capacitance of the sample capacitor and the system's stray capacitance, which was constant. The capacitor was connected to a 1-M Ω resistor to form a first-order low-pass filter, whose output was then buffered with an amplifier.

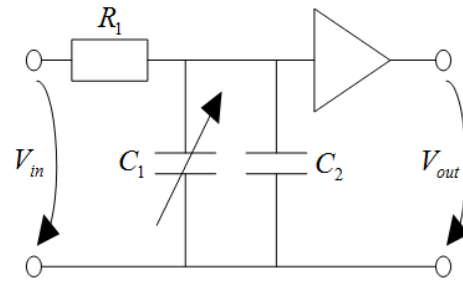


Fig. 5. First-order low-pass filter to measure the porosity of ceramics. The relative permittivity of samples affects the filter's capacitance, shown as C_1 . C_2 represents the constant stray capacitance.

The MLBS was used as an input signal. The injection was 16,383-bit long and had amplitude of 1 V. The sampling rate was 100 kHz. The input signal was injected into the system four times and (1) was used to compute the frequency response. To eliminate transience and reduce deviation in the measurements, the frequency response was calculated from the mean of the last three of those signals and their responses. The higher sampling rate could have improved system performance, but the measurement card did not enable that.

3. RESULTS AND DISCUSSION

The frequency responses of alumina ceramics with different porosities were measured. After preparation, the samples were stored in room atmosphere. Before the measurements, all samples were oven-dried at 120°C for 24 hours to remove moisture, which would have interfered with measurements. After oven-drying, the samples were placed in a desiccator, where they were allowed to cool to air temperature. In addition to ceramic samples, the measurements were carried out with air and a reference sample made of polytetrafluoroethylene (PTFE). With these reference samples, the functionality of the measurement system was verified. The calculated magnitude responses are presented in Fig. 6. In the case of ceramic samples, the presented magnitude response was a mean of five measurements with different samples from each porosity group. PTFE was also measured five times. As presented in Fig. 6, the ceramic samples gave clearly distinguishable magnitude responses.

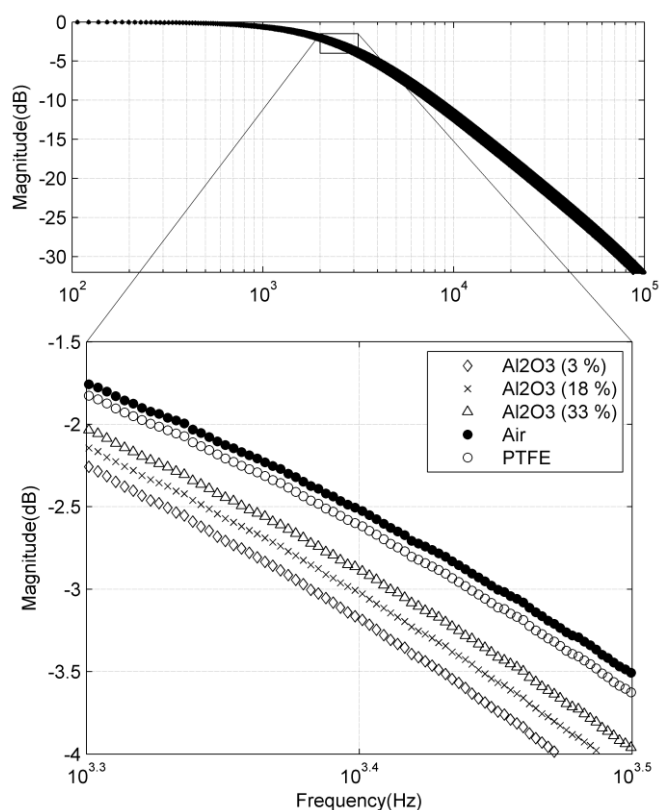


Fig. 6. Average magnitude responses of the three alumina groups having different porosities and the references, air and PTFE.

For further calculations, we chose the values of -3 dB cut-off frequencies, which are commonly used to describe the function of a low-pass filter. The system's total capacitance also can be determined from this value if resistance R is known. The total capacitance can be written as follows:

$$C = \frac{1}{2\pi Rf} \quad (3)$$

Cut-off frequencies and their standard deviations are presented in Table 3. Furthermore, an approximation of the capacitance caused by the sample was calculated. This was done by subtracting stray capacitance from the total capacitance. The stray capacitance was 55.7 pF from measurements.

Measurements of air, PTFE, and alumina produced expected results. The measurements showed that when the porosity increased, the cut-off frequency also increased, so the samples had lower capacitances. When measuring porous ceramics, there was more deviation than measuring nonporous materials such as PTFE. The porous samples were more prone to variations in air moisture and placement in the device.

Table 3. Cut-off frequencies of sample materials from magnitude responses in Fig. 6, -3 dB point, and calculated capacitances.

	Al ₂ O ₃ 3%	Al ₂ O ₃ 18%	Al ₂ O ₃ 33%	Air	PTFE
-3 dB cut-off frequency [Hz]	2412	2497	2580	2826	2759
Deviation of cut-off frequencies [Hz]	10.2	26.4	12.5	0.3	0.5
Total capacitance [pF]	66.0	63.7	61.7	56.3	57.7
Capacitance of the sample [pF]	10.3	8.1	6.0	0.7	2.0

The cut-off frequencies are presented as a function of the porosities in Fig. 7. There was a clear correlation between the magnitude response and the porosity. In addition to the relatively small measurement errors, variations were caused by the material. This is indicated by the horizontal error bars that denote the porosity variation.

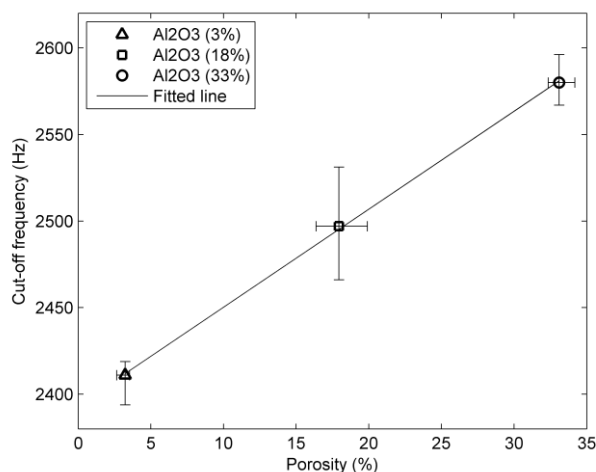


Fig. 7. Average, minimum, and maximum cut-off frequencies of each sample group, presented as a function of the total porosities from Table 1.

4. CONCLUSIONS

A frequency-response method, based on broadband excitation and Fourier techniques, was presented for characterizing porous ceramics. Series of measurements were performed with different alumina samples. The results included the cut-off frequencies, which were measured from individual ceramic samples. The relationship between the cut-off frequencies and porosities was studied.

There were three groups of samples with different porosities. The average porosities of the groups were 3 percent, 18 percent, and 33 percent. The results show that the resolution of the measurement system was sufficient to separate different porosity groups from each other. Still, the

performance of the measurement system must be increased if the system is to measure relative permittivity from different materials.

The presented frequency-response technique can be efficiently used as a non-destructive tool in online characterization of porous ceramics. Other advantages include flexibility, size scaling, and relatively simple computation algorithms required to compute the responses. Future research should study the influence of adsorbed water in porous structure on the electric frequency responses.

REFERENCES

- Ahuja, G. and Pathak K. (2009). Porous carriers for controlled/modulated drug delivery. *Indian Journal of Pharmaceutical Sciences* Vol. 71, No. 6, 599–607.
- Asmani, M., Kermel, C., Leriche, A., Ourak, M. (2001). Influence of porosity on Young's modulus and Poisson's ratio in alumina ceramics. *Journal of the European Ceramic Society* Vol. 21, 1081–1086.
- ASTM Standard C373-88, Standard test method for water absorption, bulk density, apparent porosity, and apparent specific gravity of fired whiteware products.
- Ciora, R. J. and Liu, P. K. T. (2003). Ceramic membranes for environmental related applications. *Fluid/Particle Separation Journal* Vol. 15, No. 1, 51–60.
- Coble, R. L. and Kingery W. D. (1956). Effect of porosity on physical properties of sintered alumina. *Journal of American Ceramic Society* Vol. 39, No. 11, 377–385.
- Fagan, A. J., Davies, G. R., Hutchison, J. M. S., et al. (2005). Development of a 3-D, multi-nuclear continuous wave NMR imaging system. *Journal of Magnetic Resonance* Vol. 176, No. 2, 140–150.
- Garmash, E.P., Kryuchkov, Y. N. and Pavlikov, V.N. (1995). Ceramic membranes for ultra- and microfiltration (review). *Glass and Ceramics* Vol. 52, No. 6, 150–152.
- Giesche, H. (2006). Mercury porosimetry: A general (practical) overview. *Particle & Particle Systems Characterization* Vol. 23, No. 1, 9–19.
- Godfrey, K. (1991). Design and application of multifrequency signals. *Computing & Control Engineering Journal* Vol. 2, No. 4, 187–195.
- Godfrey, K. (1993). *Perturbation Signals for System Identification*. Prentice Hall.
- James, G. (2004). *Advanced Modern Engineering Mathematics. 3rd ed.* Pearson Education Limited.
- Kamitakahara, M., Ohtsuki, C. and Miyazaki, T. (2008). Review paper: Behavior of ceramic biomaterials derived from tricalcium phosphate in physiological condition. *Journal of Biomaterials Application* Vol. 23, 197–212.
- Lira-Olivares, J., Marcano, D., Lavelle, C. and Sánchez, F. G. (2000). Determination of porosity by dielectric permittivity measurements in porous ceramics. *Revista Latinoamericana de Metalurgia y Materiales* Vol. 20, No. 2, 68–79.
- Niemelä, T., Aydogan, D. B., Hannula, M., et al. (2011). Determination of bioceramic filler distribution and porosity of self-reinforced bioabsorbable composites using micro-computed tomography. *Composites Part A: Applied Science and Manufacturing* Vol. 42, No. 5, 534–542.
- Ojuva, A., Akhtar, F., Tomsia, A. P. and Bergström, L. (2013). Laminated adsorbents with very rapid CO₂ uptake by freeze-casting of zeolites. *ACS Applied Materials & Interfaces* Vol. 5, 2669–2676.
- Pintelon, R., Schoukens, J. (2001). *System Identification: A Frequency Domain Approach*. IEEE Press.
- Richerson, D. W. (2006). *Modern Ceramic Engineering: Properties, Processing, and Use in Design*. CRC Press.
- Sanson, A., Pinasco, P. and Roncari, E. (2008). Influence of pore formers on slurry composition and microstructure of tape cast supporting anodes for SOFCs. *Journal of the European Ceramic Society* Vol. 28, No. 6, 1221–1226.
- Sing, K. S., Everett, D., Haul, R. A., et al. (1985). Reporting physisorption data for gas/solid systems with special reference to the determination of surface area and porosity. *Pure & Applied Chemistry* Vol. 57, No. 4, 603–619.
- Studart, A. R., Gonzenbach, U. T., Tervoort, E. and Gauckler, L. J. (2006). Processing routes to macroporous ceramics: A review. *Journal of the American Ceramic Society* Vol. 89, No. 6, 1771–1789.
- Sumirat, I., Ando, Y. and Shimamura, S. (2006). Theoretical consideration of the effect of porosity on thermal conductivity of porous materials. *Journal of Porous Materials* Vol. 13, No. 3–4, 439–443.
- Taud, H., Martinez-Angeles, R., Parrot, J. F. and Hernandez-Escobedo, L. (2005). Porosity estimation method by X-ray computed tomography. *Journal of Petroleum Science and Engineering* Vol. 47, No. 3–4, 209–217.
- Vasiliev, P. O., Ojuva, A., Grins, J. and Bergström, L. (2010). The effect of temperature on the pulsed current processing behaviour and structural characteristics of porous ZSM-5 and zeolite Y monoliths. *Journal of the European Ceramic Society* Vol. 30, No. 14, 2977–2983.
- Vila, R., Gonzalez, M., Molla, J. and Ibarra, A. (1998). Dielectric spectroscopy of alumina ceramics over a wide frequency range. *Journal of Nuclear Materials* Vol. 253, 141–148.